Acta Pharmacologica Sinica

www.nature.com/aps

ARTICLE

New monoamine antidepressant, hypidone hydrochloride (YL-0919), enhances the excitability of medial prefrontal cortex in mice via a neural disinhibition mechanism

Yong-mei Zhang[1,2], Lu-yu Ye[1,2], Tian-yu Li[1,2], Fan Guo[1,2], Fei Guo[1,2], Yang Li[1,2] and Yun-feng Li[3]

Hypidone hydrochloride (YL-0919) is a novel antidepressant in clinical phase II trial. Previous studies show that YL-0919 is a selective 5-HT (serotonin) reuptake inhibitor, 5-HT_{1A} receptor partial agonist, and 5-HT_6 receptor agonist, which exerts antidepressant effects in various animal models, but its effects on neural function remain unclear. Medial prefrontal cortex (mPFC), a highly evolved brain region, controls highest order cognitive functions and emotion regulation. In this study we investigated the effects of YL-0919 on the mPFC function, including the changes in neuronal activities using electrophysiological recordings. Extracellular recording (in vivo) showed that chronic administration of YL-0919 significantly increased the spontaneous discharges of mPFC neurons. In mouse mPFC slices, whole-cell recording revealed that perfusion of YL-0919 significantly increased the frequency of sEPSCs, but decreased the frequency of sIPSCs. Then we conducted whole-cell recording in mPFC slices of GAD67-GFP transgenic mice, and demonstrated that YL-0919 significantly inhibited the excitability of GABAergic neurons. In contrast, it did not alter the excitability of pyramidal neurons in mPFC slices of normal mice. Moreover, the inhibition of GABAergic neurons by YL-0919 was prevented by pre-treatment with 5-HT_{1A} receptor antagonist WAY 100635. Finally, chronic administration of YL-0919 significantly increased the phosphorylation levels of mTOR and GSK-3β in the mPFC as compared with vehicle. Taken together, our results demonstrate that YL-0919 enhances the excitability of mPFC via a disinhibition mechanism to fulfill its rapid antidepressant neural mechanism, which was accomplished by 5-HT_{1A} receptor-mediated inhibition of inhibitory GABAergic interneurons.

Keywords: YL-0919; medial prefrontal cortex; GABAergic neurons; 5-HT_{1A} receptor; GAD67-GFP transgenic mice; disinhibition; fluoxetine; electrophysiological recording

Acta Pharmacologica Sinica (2022) 43:1699–1709; https://doi.org/10.1038/s41401-021-00807-0

INTRODUCTION

Major depressive disorder (MDD) is one of the most common and recurring mental illness among the leading contributors to social and economic burden worldwide [1, 2]. The clinical symptoms of MDD include anhedonia, lack of energy, dysfunction of cognition and memory, and a high rate of suicide [3]. In the past few decades, selective 5-HT (serotonin) reuptake inhibitors were widely used as antidepressants. However, they have several side effects, including sexual dysfunction, weight gain, and lag to produce a therapeutic response [4, 5]. The slow-onset of action of the monoamine antidepressants [6] and their side effects require an urgent need to develop more rapid and reliable antidepressants, and stimulate interests of exploring the neural mechanisms underlying these rapid antidepressant effects and the pathophysiology of MDD [7–9].

Medial prefrontal cortex (mPFC) is a highly evolved brain region and controls highest order cognitive abilities and emotion regulation [10]. The studies on both human and rodents with depressive phenotypes displayed structural and functional impairments of mPFC, such as the dendritic atrophy [11–13] and dysfunction of network connections [14]. The neurophysiological mechanism studies reported that the rodents with depressive phenotype exhibit a reduction of E/I balance in the mPFC and hypoexcitability of the mPFC [15]. Brain stimulation and imaging studies in humans have highlighted a key role for the prefrontal cortex in clinical depression [16, 17]. However, it remains unclear whether excitation or inhibition of prefrontal cortical neuronal activity is associated with monoamine antidepressants.

Recently, a novel antidepressant in clinical trial II, hypidone hydrochloride (YL-0919), exhibited effects of selective 5-HT reuptake inhibition, partial 5-HT_{1A} receptor agonists and 5-HT_6 receptor agonists [18, 19] (Fig. 1a). Our previous studies showed that YL-0919 displayed a significant antidepressant effect on several types of depressive animal models [18, 20–22], and more rapid onset time than fluoxetine and vilazodone. YL-0919 also displayed memory-enhancing effect in behaviors of Morris water maze [19]. Although there are several pharmacological reports about YL-019, the underlying neural mechanism of YL-0919 is still lacking, especially the impact of YL-0919 on the mPFC needs to be further explored.

[1]CAS Key Laboratory of Receptor Research, Center for Neurological and Psychiatric Research and Drug Discovery, Shanghai Institute of Materia Medica, Chinese Academy of Sciences, Shanghai 201203, China; [2]University of Chinese Academy of Sciences, Beijing 100049, China and [3]Beijing Institute of Pharmacology and Toxicology, State Key Laboratory of Toxicology and Medical Countermeasures, Beijing Key Laboratory of Neuropsychopharmacology, Beijing 100850, China
Correspondence: Fei Guo (guofei@simm.ac.cn) or Yang Li (liyang@simm.ac.cn) or Yun-feng Li (lyf619@aliyun.com)

Received: 22 April 2021 Accepted: 28 October 2021
Published online: 22 November 2021

In the present study, by using in vivo electrophysiological recordings, we investigated the effect of YL-0919 on the mPFC function, including the changes in neuronal activities. After confirming the enhancement of YL-0919 in the activities of mPFC, we further explored the neural mechanism of YL-0919 by multiple functional recording and genetic labeling of GABAergic interneurons. Our results indicated that YL-0919 increases the activities of the mPFC not by directly acting on excitatory pyramidal neurons, but through a strong inhibition on the inhibitory GABAergic interneurons, and 5-HT_{1A} receptor may be an important regulator during this process. Therefore, as a promising antidepressant, YL-0919 exhibits a novel neural mechanism that converges the monoamine antidepressants and the regulation of E/I balance.

MATERIALS AND METHODS

Animals

All the procedures were followed the National Institutes of Health's Guide for the Care and Use of Laboratory Animals and were approved by the Animal Care Committees of Shanghai Institute of Materia Medica, Chinese Academy of Sciences on the protection of animals used for scientific purposes. Adult male C57BL/6 mice (20–22 g, 6–8 weeks old) after chronic drug administration were used for the proceeding of electrophysiology recording in vivo and ex vivo. C57BL/6 mice aged 15–20 days were used for electrophysiology in acute slices. The GAD67-GFP mice were obtained from Institute of Neuroscience, Chinese Academy of Sciences. The mice were housed (5 mice per cage) in temperature-controlled rooms with standard 12 h light/dark cycles and food and water were available *ad libitum*. Each operation was taken to minimize stress and the number of animals used in each series of experiments.

Behavioral test

The mice were randomly divided into three groups and were treated with YL-0919 (2.5, 10 mg/kg, intragastric administration (i.g.)), fluoxetine (2.5, 10 mg/kg, intraperitoneal injection (i.p.); TCI, CAS RN: 56296-78-7), or saline (i.g.). The behavioral tests (10 animals per group), including the force swimming test (FST) and open field test (OFT), were performed after 1 day, 1 week, or 2 weeks of drug treatment [23]. The dose of YL-0919 was chosen based on our previous studies, and the vehicle or fluoxetine was administered by i.g. In the behavioral experiments; the investigators were blinded to the treatment of the mice.

Force swimming test. The FST was conducted in normal light as previously described [24]. Briefly, mice were individually placed in a cylinder of water. The cylinders (35 cm height × 10 cm diameter) were set to prevent mice from touching the bottom with their limbs. Water temperature was maintained at 23–24 °C. Mice were allowed to swim for 10 min at least 1 day before normal experiments were performed. During experiments, mice were allowed to swim for 6 min, and their activity was videotaped. The duration of immobility defined as floating or remaining motionless was assessed for the last 4 min.

Open field test. The OFT is a standard method to profile locomotor activity. Briefly, the mice were comforted and placed in the center of a square box (size: 35 cm × 35 cm × 45 cm) that was made of white acrylic plastic. Mice were allowed to explore the box for 10 min and were monitored online. The moving trail and velocity for each animal were calculated offline.

In vivo electrophysiology

The adult male C57BL/6 mice received 2-week administration of drugs, which included: YL-0919 in saline, fluoxetine in saline and vehicle (saline). The electrophysiological recording was procedure after the animals were rested for 1 day. Before surgeries, the animals were anesthetized with pentobarbital sodium (80 mg/kg, i.g.). Then, the anesthetized mice were mounted on a stereotaxic apparatus (Narishige, Tokyo, Japan) for single-unit extracellular recording. The skull and the dura overlying the mPFC were removed after the mice were anesthetized and stable. The electrodes pulled from 1.5 mm (o.d.) borosilicate glasses were used to record the current in the mPFC (1.5–1.9 mm anterior to bregma, 0.5–0.9 mm lateral to the midline, 1.5–2.5 mm depth under the cortical surface). The electrodes were filled with 2 M NaCl (Sigma) and 0.5% Chicago sky blue (Sigma) solution.

Single-unit extracellular recording was carried out to confirm the firing rate and pattern of pyramidal cells in mPFC [25]. Two types of activities of pyramidal neurons were recorded spontaneously in the mPFC. The burst firing had a positive-skewed distribution of interspike interval histogram (ISIH) with a long progressive decline (Fig. 1j). The single-spike firing was firing in irregular single spikes with a nearly symmetrical ISIH (Fig. 2b). We detected the burst firing cited from Legendy and Salcman [26], who use Poisson surprise method by finding successive interspike intervals (ISIs) that are less than half the mean ISI of the entire spike train. The pentobarbital sodium was injected to maintain the anesthesia during the surgery and the electrophysiological recording. Body temperature was maintained at 37 ± 0.5 °C using a thermostatically controlled heating pad (ATC1000; WPI).

Whole-cell electrophysiology

Preparing for the acute slices. The mice were anaesthetized with pentobarbital sodium (80 mg/kg, i.p.) and then perfused with 20–40 mL of ice-cold and pre-oxygenated artificial cerebrospinal fluid (ACSF) (in mM): 120 NaCl, 2.5 KCl, 26 $NaHCO_3$, 1 NaH_2PO_4, 10 D-glucose, 1.3 $MgCl_2$, and 2.5 $CaCl_2$, gassed with 95% CO_2 and 5% CO_2. The brain was immediately dissected out to 300-μm thick slices containing the mPFC after decapitation, using a vibratome (Leica VT1000s, Wetzlar, Germany). And then, the mPFC slices were quickly transferred to the recovering chamber and incubated in normal ACSF at 28 °C for 1 h and gassed with 95% O_2 and 5% CO_2. Finally, the slices were transferred to the recording dish at room temperature for recording.

Electrophysiology recording. All the recordings on the mPFC slices were performed using a MultiClamp 700B amplifier (Molecular Device, San Jose, USA) under an Olympus microscope (Olympus, Japan) equipped with infrared differential interference contrast optics. For the recording of spontaneous excitatory postsynaptic current (sEPSC), spontaneous inhibitory postsynaptic current (sIPSC), and the action potentials (APs) of pyramidal neurons, the pyramidal neurons in layer V were recognized by characteristic pyramidal shape. Briefly, recordings were performed in ACSF containing (in mM): 120 NaCl, 2.5 KCl, 26 $NaHCO_3$, 1 NaH_2PO_4, 10 D-glucose, 1.3 $MgCl_2$, and 2.5 $CaCl_2$, gassed with 95% O_2 and 5% CO_2. All the resistance of glass electrodes were controlled in the range of 3–8 MΩ. The intracellular solution for EPSC recording contained (in mM): 115 $CsMeSo_3$, 20 CsCl, 10 HEPES, 2.5 $MgCl_2$, 4 Na_2-ATP, 0.4 Na-GTP, 10 Na-phosphocreatine, 0.6 EGTA (pH = 7.35). The intracellular solution for IPSC recording contained (in mM) 110 CsCl, 30 K-gluconic acid, 0.1 $CaCl_2$, 10 HEPES, 4 Mg-ATP, 0.3 GTP, 1.1 EDTA, and pH was adjusted to 7.3 with KOH. The intracellular solution for AP recording contained (in mM) 120 K gluconate, 20 KCl, 4 Na_2-ATP, 0.3 Na-GTP, 5 Na-phosphocreatine, 0.1 EGTA, 10 HEPES (pH = 7.2). For recording EPSCs at −60 mV, the bicuculline (10 μM) was added to ACSF; for recording IPSCs at −80 mV, CNQX (20 μM) and MK-801(10 μM) were added to ACSF. For recording APs, the current-clamp was performed. APs in pyramidal neurons and GABAergic neurons were driven by step-current injection of 0–350 pA, and the trial length for 1 run was 8 sweeps of 500 ms. Membrane currents (voltage-clamp) and membrane potentials (current-clamp) were acquired at 50 and 20 kHz

sampling frequency, respectively, using Digi data 1440 A (Molecular Devices, USA), after low-pass filtering at 2 kHz with the Bessel filter built-into the EPC-10 amplifier. The data of EPSCs and IPSCs were analyzed by the Mini Analysis Program (Synaptosoft), and the data of APs were analyzed by the Clampfit 10.7.

Multiplex fluorescence in situ hybridization

Mice were perfused intracardially with DEPC-PBS followed by ice-cold 4% PFA in PBS. Brains were dissected and post-fixed in 4% PFA for 12–24 h at 4 °C and dehydrated with 30% sucrose in DPEC-PBS. Afterward, the brains were cut coronally at 20 μm with cryotome and mounted to SuperFrost Plus® Slides (Thermo Fisher Scientific, USA). After drying in the air, slides were stored in −80 °C for up to 1 month. Tissue sections were then dried in the ACD hybridizer at 37 °C for at least 1 h, treated with hydrogen peroxide for 10 min, and dried before protease treatment at 60 °C for 30 min. The boiling step in the antigen-retrieval procedure has been omitted and the sections were digested in Protease Plus (Advanced Cell Diagnostics, Inc.) solution for 15 min at 40 °C. Each RNA signal has been developed sequentially by specifically targeting each probe with horseradish peroxidase, which converted fluorescently labeled tyramide (TSA Plus fluorescein, Cy3 or Cy5 kit, PerkinElmer) into an insoluble stain around the RNA of interest. The final concentration of tyramide in TSA buffer solution was 1:1500. Custom RNAscope target probes (all targeting mouse transcripts) against Htr1a mRNA (Probe-Mm-Htr1a, Cat No. 312301, ACDBio), Slc32a1 mRNA (Probe-Mm-Slc32a1-C3, Cat No. 319191-C3, ACDBio), Htr6 mRNA (Probe-Mm-Htr6, Cat No. 411161, ACDBio), and Slc17a7 mRNA (Probe-Mm-Slc17a7-C2, Cat No. 416631-C2, ACDBio) were ordered from ACDBio and used in the experiment. Images were captured under a ×10 or ×60 objective using a confocal microscope (Lecia TCS SPS CFSMP, Germany).

Western blot

Western blot was carried out to clarify the molecular basis for the neuronal mechanisms of YL-0919. The protein expressions of mTOR and GSK-3β in the mPFC were examined in mice after chronic administration of drugs. One day after chronic drugs administration, mice were anaesthetized with pentobarbital sodium (80 mg/kg, i.p.). The mPFC regions were immediately extracted after decapitation. The tissue was dissected and immediately homogenized in ice-cold homogenization buffer (in mM, 0.5 dithiothreitol, 1 EDTA, 2 EGTA, 10 HEPES, 0.1 PMSF, 10 mg/L leupeptin, and 2 mg/L aprotinin). The total protein concentrations were determined using the bicinchoninic acid assay (Pierce, Rockford, IL, USA). A portion of whole homogenate was centrifuged at 14,000 × *g* for 10 min and the protein samples were obtained, and the protein samples were resuspended in boiling 1% sodium dodecyl sulfate and stored at −80 °C. The primary and the secondary antibodies used included: anti-mTOR (1:1000, Cell Signaling Technology, #2983s), anti-p-mTOR (1:1000, Cell Signaling Technology, #2971s), anti-GSK-3β (1:1000, Cell Signaling Technology, #9315s), anti-p-GSK-3β (1:1000, Cell Signaling Technology, #5558s), anti-β-actin (1:1000, Cell Signaling Technology, #8457), and goat anti-rabbit IgG (1:5000, Abcam, ab6721). The density of each band on Western blot was measured using Image Processing and Analysis in Java (ImageJ) software, and the relative expression level of each target protein was calculated as the ratio of target protein band density to β-actin density (the loading control).

Statistical analysis

Statistical analysis was performed in a manner blinded to treatment assignments in all behavioral experiments using GraphPad Prism software v7 and Origin 8. The data were expressed as the mean ± standard error of mean (SEM). All statistical tests were two-tailed, and significance was assigned at $P < 0.05$. Normality and equal variances between group samples were assessed using the D'Agostino and Pearson omnibus normality test and Bartlett's test, respectively. When normality and equal variance between sample groups was achieved, one-way ANOVA (followed by Dunnett's post hoc test), or *t*-test was used. Where normality or equal variance of samples failed, Kruskal–Wallis one-way ANOVA (followed by Dunn's correction) or Mann–Whitney *U* test was performed. Two-way ANOVA (followed by Sidak's multiple comparisons test) was used in appropriate situations. The χ^2 test of independence was used to assess the proportion of neurons fired in bursts. Cumulative probability was analyzed by Kolmogorov–Smirnov test. The sample sizes, specific statistical tests were used, and main effects of our statistical analyses for each experiment are reported in Supplementary Table S1. The significance of cumulative probability distributions was defined as $P < 0.05$, $P < 0.01$, $P < 0.001$. $P \geqq 0.05$ were considered not significant (ns).

RESULTS

YL-0919 exhibited anti-depressive effects and enhanced the excitability of the mPFC in vivo

The FST and OFT were used to measure anti-depressive effect of YL-0919. After chronic treatment with YL-0919 (2.5 mg/kg, Supplementary Fig. S1a) once a day for consecutive 7 or 14 days, the immobility time in FST was significantly decreased compared with vehicle (saline) (Fig. 1c, d), while fluoxetine (10 mg/kg, Supplementary Fig. S1a) decreased the immobility time after 14 days administration (Fig. 1c, d). In the OFT (Fig. 1e), the total movement distance was not changed by the chronic treatment with YL-0919, suggesting that the locomotor activity was not affected (Fig. 1f–h). These data confirmed that YL-0919 exerted significant antidepressant effect in mice.

To investigate the neural mechanism underlying the antidepressant effect of YL-0919, we performed in vivo functional recordings in the mPFC of chronicly treated mice. The in vivo extracellular electrophysiological recordings showed that the activities of pyramidal cells in the mPFC were significantly enhanced after chronic administration of YL-0919, compared to vehicle group (saline) (Fig. 1i–l). We further analyzed two firing patterns of pyramidal neurons, including burst spike firing and single-spike firing patterns in mPFC (Fig. 1j), and found that single-spike firing rates of pyramidal cells were significantly increased (Fig. 1k), indicated that YL-0919 could increase the neuronal activities of pyramidal neurons in the mPFC.

YL-0919 enhanced excitatory transmission and reduced inhibitory transmission in the mPFC

To investigate whether YL-0919 has a direct effect on the neurotransmission of the mPFC, we measured the sEPSCs and sIPSCs of layer V pyramidal neurons in mPFC slices by patch-clamp recordings ex vivo. The frequency of sEPSCs was increased by the perfusion of YL-0919, and there was no significant change of the amplitude of sEPSCs (Fig. 2a–c and Supplementary Fig. S2a, b). The recordings of the sIPSCs of pyramidal neurons displayed that the frequency of sIPSCs was significantly decreased after perfused with YL-0919 in the recording chamber (Fig. 2d–f and Supplementary Fig. S2c, d). We also tested the effect of different concentrations of YL-0919 on sEPSCs and sIPSCs; the dose at which YL-0919 started to exert effect was 20 μM (Supplementary Fig. S2). We then recorded the effect of YL-0919 on the miniature excitatory postsynaptic currents (mEPSCs) and the miniature inhibitory postsynaptic currents (mIPSCs) by adding TTX into bath solution to block the AP evoked currents. Our results showed that YL-0919 exhibited no significant effect on the mEPSCs and mIPSCs of pyramidal neurons (Supplementary Fig. S3), demonstrating that YL-0919 may mainly affect the firing inputs to pyramidal neurons driven by APs. The above results indicated that YL-0919 perfusion increases the excitatory input and decreases the inhibitory input to pyramidal neurons in the mPFC.

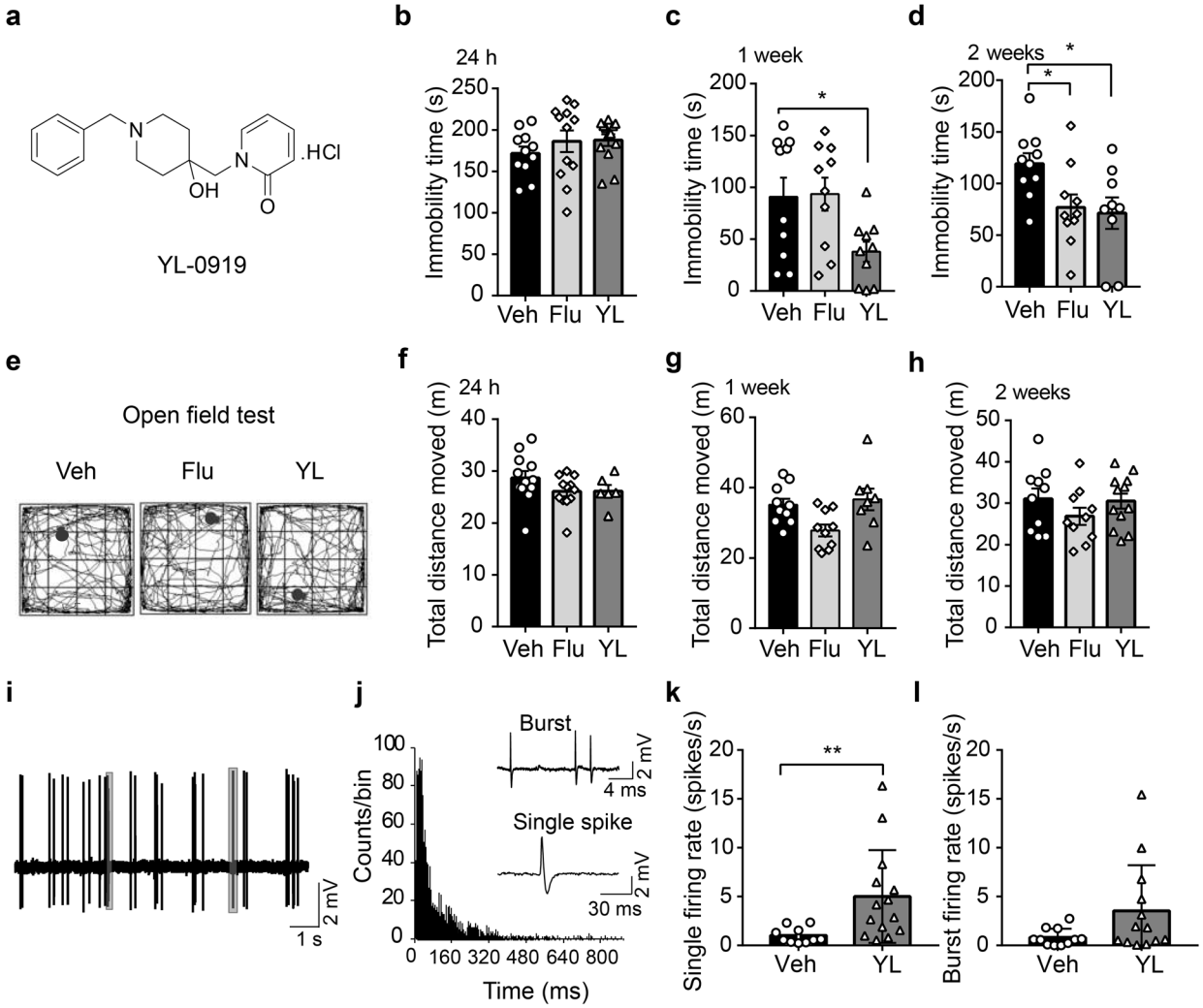

Fig. 1 YL-0919 treatment produced antidepressant effects and increased the neuronal activities of pyramidal neurons in the mPFC. a The chemical structure of YL-0919. **b**–**d** The immobility times measured in the force swimming test (FST) after administration of vehicle (Veh, i.g.), fluoxetine (Flu, i.p.), and YL-0919 (YL, i.g.) for 1 day (**b**), 1 week (**c**), and 2 weeks (**d**), and the data showed that YL-0919 significantly decreased the immobility time compared with vehicle-treated group after 1- and 2-week of treatment. $n = 10$–13 mice per group. **e** The schematic diagram of open field test (OFT). **f**–**h** The total distance moved in the OFT showed no significant changes after 1-day (**f**), 1-week (**g**), and 2-week (**h**) intragastric administration of vehicle/fluoxetine/YL-0919. $n = 10$–13 mice per group. **i** The in vivo recording traces of spike firing in the mPFC. $n = 5$ rats per group. **j** The sample traces of burst spike firing (top) and single-spike firing (middle) and the characteristic histogram distribution of pyramidal neurons (bottom). **k** YL-0919 significantly increased the single-spike firing rate of pyramidal neurons in the mPFC compared with vehicle. **l** YL-0919 slightly increased the burst spike firing rate of pyramidal neurons in the mPFC. Data are presented as mean ± SEM, statistics are measured by one-way ANOVA followed by Dunnett's *post hoc* test (**b**, **c**, **d**, **f**, **g**, **h**) and unpaired *t*-test (**k**, **l**), $^{*}P < 0.05$; $^{**}P < 0.01$. See Supplementary Table S1 for all statistical analysis and *n* numbers.

YL-0919 strongly inhibited action potentials of GABAergic neurons in mPFC

The above findings led us to investigate the direct effect of YL-0919 on the pyramidal neurons and GABAergic interneurons, respectively. We conducted the whole-cell patch-clamp recordings of layer V pyramidal neurons in the mPFC slices and evaluated the effect of YL-0919 on intrinsic excitability (Fig. 3a). We recorded the APs evoked by a sequence of current injections, and found that YL-0919 had no significant effect on the firing rate and threshold of APs and rest membrane potentials of pyramidal neurons and the AP amplitude (Fig. 3b–h and Supplementary Fig. S4). These results exhibited that YL-0919 had no significant influence on the intrinsic excitability of pyramidal neurons.

To identify the GABAergic neurons, we used GAD67-EGFP-labeled mice. These transgenic mice selectively expressed enhanced green fluorescent protein (EGFP) under the direction of the mouse Gad1 (glutamic acid decarboxylase 1 or GAD67) promoter in GABAergic neurons (Fig. 3i). Then we conducted whole-cell patch-clamp recordings on GABAergic neurons in the mPFC coronal slices, and measured the current-evoked APs in GABAergic neurons. Surprisingly, YL-0919 perfusion significantly inhibited the APs of GABAergic neurons (Fig. 3j–o), especially the spiking numbers and the frequency at 250 pA current input were markedly reduced by YL-0919 (Fig. 3j–l). These data showed that YL-0919 had a significant inhibition on the membrane excitability of GABAergic neurons, rather than directly on pyramidal neurons, suggesting an important role of GABAergic neurons in the mPFC underlying the antidepressant effect of YL-0919.

Inhibition of GABAergic neurons by YL-0919 was blocked by the pharmacological inactivation of 5-HT_{1A} receptor

Our previous studies have shown that YL-0919 is a 5-HT_{1A} receptor partial agonist and a 5-HT_6 receptor agonist [19]. The 5-HT_{1A} receptor and 5-HT_6 receptor are widely distributed in the mPFC

[27, 28]. We confirmed the expression of 5-HT_{1A} receptor or 5-HT_6 receptor on the pyramidal neurons and GABAergic neurons in the mPFC. The immunological co-localization results showed that 5-HT_{1A} receptors were abundantly expressed on both pyramidal neurons and GABAergic neurons in the mPFC (Fig. 4a). And 5-HT_6 receptors were widely expressed on the pyramidal neurons, while less of 5-HT_6 receptors colocalized with GABAergic neurons compared with 5-HT_{1A} receptors (Fig. 4b).

Then, to further explore how YL-0919 inhibited the membrane excitability of GABAergic neurons, we performed the recordings by pharmacological inhibition of 5-HT_{1A} receptor and 5-HT_6 receptor, respectively. The 5-HT_{1A} receptor antagonist (10 μM WAY 100635 [29, 30]) was pre-perfused to the recording chamber prior to YL-0919, and the results demonstrated that WAY 100635 completely prevented the inhibition of GABAergic neurons by YL-0919 (Fig. 5a–d). While the 5-HT_6 receptor antagonist (5 μM SB217046 [31]) could not eliminate the YL-0919-induced reduction of GABAergic firings (Fig. 5e–h). These results indicated that 5-HT_{1A} receptors played an important role for the inhibition of the GABAergic neurons by YL-0919.

YL-0919 activated synaptic-related signaling pathway

Since functional antidepressant effect is correlated with protein expression and intracellular signaling pathway [32], to further identify the influence of YL-0919 on the synaptic-related signaling pathway in the mPFC, we analyzed the expression of mTOR and GSK-3β protein and their phosphorylation in the mPFC by Western blotting methods. Our results showed that YL-0919 treatment (2.5 mg/kg per day) significantly upregulated the phosphorylation levels of mTOR and GSK-3β in the mPFC compared with vehicle (Fig. 6a, b). In contrast, the levels of p-GSK-3β were only increased by 14-day treatment of fluoxetine (Fig. 6d). The results indicated that YL-0919 treatment could significantly increase the expression of neurogenesis related proteins, which in turn exerted an enhancement in synaptic function in the mPFC.

DISCUSSION

Previous studies have displayed the antidepressant effect of YL-0919 in different animal models, but its neural mechanism in the mPFC is unclear. In the present study, we investigated the neural effect of YL-0919 in the mPFC and the neural mechanism underlying its anti-depressive effect. Our results showed that chronic administration of YL-0919 significantly increased the neuronal activity of pyramidal neurons and the phosphorylation of mTOR and GSK-3β in the mPFC. More importantly, our results demonstrated that YL-0919 could preferentially inhibit the APs of GABAergic neurons, which reduced the tonic inhibitory output on pyramidal neurons and led to a broadly excitation of neurons in mPFC. Finally, pharmacological blockade by antagonist of 5-HT_{1A} receptor could prevent the inhibition of GABAergic neurons by YL-0919. These findings demonstrate that YL-0919 may preferentially exert inhibition on GABAergic interneurons through activation of 5-HT_{1A} receptor, and lead to the enhancement of mPFC excitability through a “disinhibition” mechanism.

Previous studies have demonstrated that the mPFC is one of the important brain regions for decision making and emotional controls, also correlates well with the symptoms and treatment of depression. Guo et al. reported that fluoxetine and a rapid antidepressant candidate, YY-23, could reverse depression-like behavior in rats induced by chronic stress, and rescue the decreased activity of pyramidal neuron in mPFC [25]. These results suggested that the activity of pyramidal neurons in the mPFC is correlated well with depressive-like behaviors. Lei et al. found that deletion of SIRT1 (Sirtuin1, a key regulator of cellular metabolism) could inhibit the intrinsic excitability of layer V pyramidal neurons

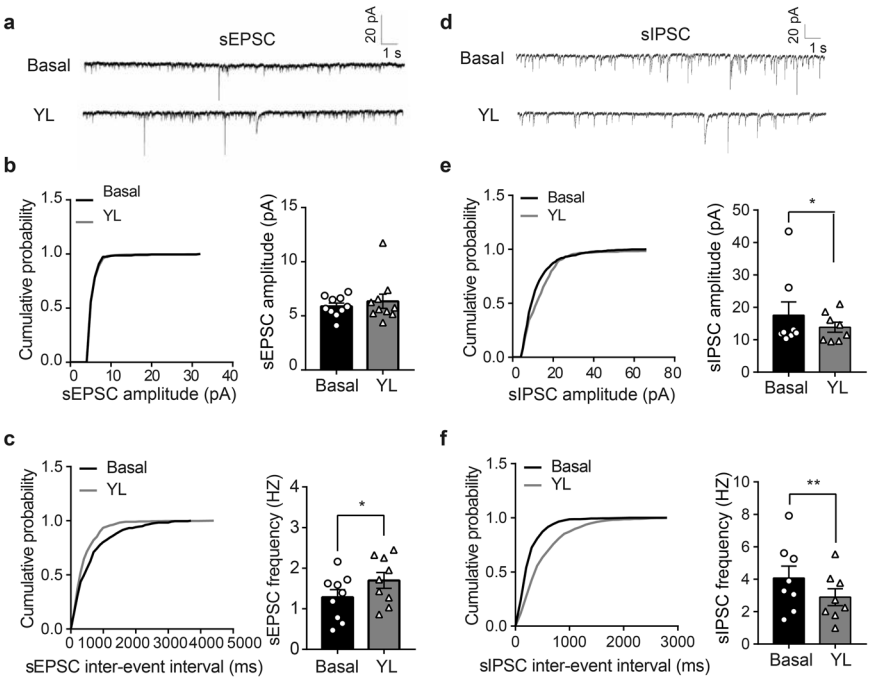

Fig. 2 YL-0919 perfusion increased the frequency of sEPSCs and decreased frequency of sIPSCs in the mPFC. a Representative traces of sEPSCs in basal condition and YL-0919 perfusion. **b** Cumulative probability of sEPSC amplitude and averaged amplitude showed no significant influence after YL-0919 perfusion. **c** Cumulative probability of sEPSC inter-event interval and averaged frequency, and the results showed a significant increase in the frequency of sEPSCs by YL-0919. $n = 10$ neurons from 4 mice. **d** Representative traces of sIPSCs of basal condition and YL-0919. **e** Cumulative probability of sIPSC amplitude and averaged amplitude showed no significant changes in YL-0919. **f** Cumulative probability of sIPSC inter-event interval and averaged frequency, the results showed a significant decrease in the frequency of sIPSCs in YL-0919 group. $n = 8$ neurons from 4 mice. Statistics are measured by nonparametric K–S test (left: **b**, **e**, **c**, **f**) and one-way ANOVA followed by Dunnett's *post hoc* test (right: **b**, **e**, **c**, **f**), $^*P < 0.05$; $^{**}P < 0.01$.

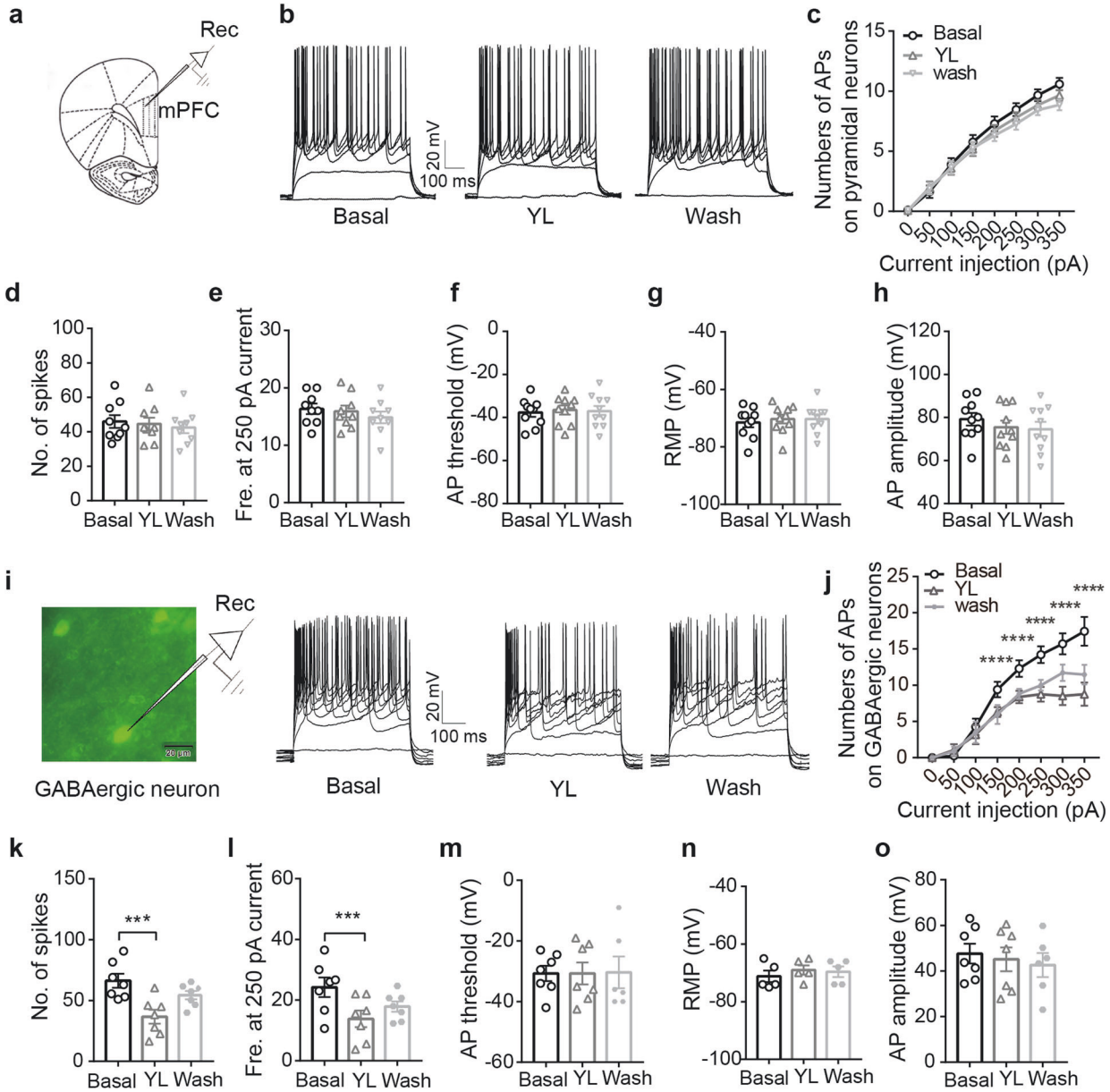

Fig. 3 YL-0919 perfusion preferentially inhibited the membrane excitability of GABAergic neuron in the mPFC slices. a The scheme of recordings in the mPFC. **b** Representative traces in the presence of ACSF (Basal, left), 20 μM YL-0919 (middle) and wash out (right) at 0–350 pA currents input in steps of 50 pA. APs were recorded in nine cells from three biologically independent mice per group. **c** Numbers of action potentials (APs) fired on the pyramidal neurons showed no change after YL-0919 perfusion. **d**–**h**. Comparisons of numbers of spikes (**d**), frequency at 250 pA current input (**e**), AP threshold (**f**), and resting membrane potential (RMP) (**g**), all index showed no significant changes when bath perfused with 20 μM YL-0919 (**h**). **i** The schematic diagram of patching a GABAergic neuron labeled by EGFP in the mPFC of transgenic mice ex vivo (left). Representative traces in the presence of ACSF (Basal), 20 μM YL-0919 and wash out at 0–350 pA currents input in steps of 50 pA (right). Traces were recorded from ten cells from four biologically independent mice per group, with similar results obtained. **j** Numbers of APs fired in the GABAergic neurons were decreased after perfusing with YL-0919 compared with basal. **k**–**o** Comparisons of numbers of spikes (**k**), frequency at 250 pA current input (**l**), AP threshold (**m**), RMP (**n**), and AP amplitude (**o**), YL-0919 significantly inhibited the firing rates of the GABAergic interneurons, including numbers of spikes (**k**) and frequency at 250 pA current input (**l**). Data are presented as mean ± SEM. Statistics are measured by two-way ANOVA followed by Turkey's *post hoc* test (**c**, **j**) and paired *t*-test (**d**, **e**, **f**, **g**, **h**, **k**, **l**, **m**, **n**, **o**), $^{*}P < 0.05$; $^{**}P < 0.01$, $^{***}P < 0.001$, $^{****}P < 0.0001$.

and decreased the spontaneous excitatory synaptic transmission in mPFC, which resulted in depression-like behavior in mice [33]. And SIRT1 activator (SRT2104) reversed anhedonia and behavioral despair and increased the activities of pyramidal neurons in a mice model with chronic unpredictable mild stress [33]. Hare et al. utilized optogenetic techniques to demonstrate that light activation of dopamine type 1 receptor (DRD1) expressing pyramidal neurons produced rapid and long-lasting antidepressant effects, and disruption of DRD1 activity also blocked the rapid antidepressant effects of ketamine [34]. These studies suggested that increasing the excitability of mPFC may be a potential mechanism to generate rapid antidepressant. Our studies found that YL-0919 not only significantly enhanced the activity of pyramidal neurons in the mPFC (Fig. 1), but also enhanced the excitatory synaptic transmission and decreased inhibitory synaptic transmission of mPFC in brain slice (Fig. 2), suggesting that the enhancement of

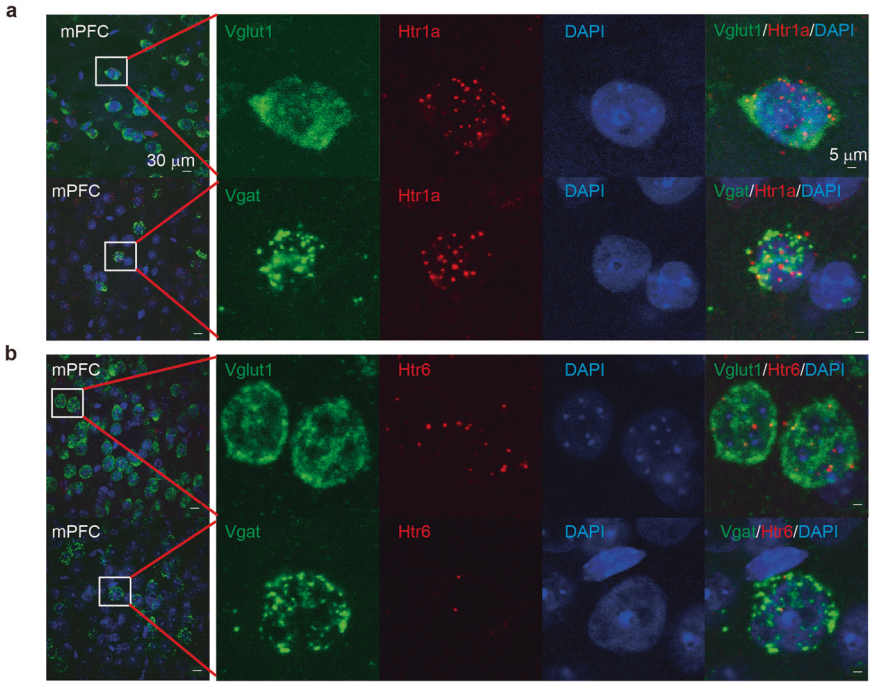

Fig. 4 5-HT$_{1A}$ receptors were widely distributed on both pyramidal neurons and GABAergic neurons, while 5-HT$_6$ receptors were mainly distributed on pyramidal neurons in the mPFC. a Representative confocal immunofluorescent images of the mPFC pyramidal neurons or GABAergic interneurons with 5-HT$_{1A}$ receptors (Htr1a, red); the results showed that 5-HT$_{1A}$ receptors were abundantly distributed on both pyramidal neurons (top) and GABAergic neurons (bottom). Vglut1(green): a sign of pyramidal neuron. Vgat (green) showed GABAergic interneuron. Scale bar in **a** left = 30 μm, right = 5 μm. **b** Representative confocal immunofluorescent images of the mPFC pyramidal neurons or GABAergic interneurons with 5-HT$_6$ receptors (Htr6, red); the results showed that 5-HT$_6$ receptors were widely distributed on the pyramidal neurons (top), but a few of 5-HT$_6$ receptors were distributed on the GABAergic neurons (bottom). Vglut1 (green): a sign of pyramidal neuron. Vgat (green) showed GABAergic interneuron. Scale bar in a left = 30 μm, right = 5 μm.

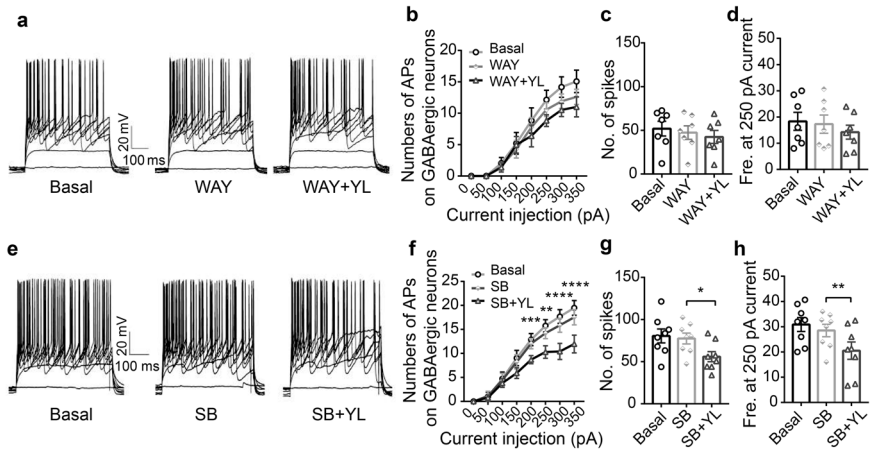

Fig. 5 5-HT1A receptor antagonist, WAY 100635, prevented the inhibition of GABAergic neuron induced by YL-0919, while 5-HT6 receptor antagonist, SB271046, could not block the inhibition of GABAergic neuron induced by YL-0919. a Representative traces in the presence of basal (ACSF), 10 μM WAY 100635 and 10 μM WAY 100635 with 20 μM YL-0919 at 0–350 pA currents input in steps of 50 pA. **b** Numbers of AP fired at 0–350 pA currents input in steps of 50 pA. **c** Comparisons of spike numbers. **d** Comparisons of frequency at 250 pA current input. $n = 7$ neurons from three mice. **e** Representative traces in the presence of basal (ACSF), 5 μM SB 271046 and 5 μM SB 271046 with 20 μM YL-0919 at 0–350 pA currents input in steps of 50 pA. **f** Numbers of AP fired at 0–350 pA currents input in steps of 50 pA, the results suggested that YL-0919 significantly inhibited the AP firing of GABAergic neurons in the presence of SB271046. **g** Comparisons of all AP numbers showed that SB271046 could not significantly block the inhibition of GABAergic neurons by YL-0919. **h** Comparisons of 250 pA current frequency exhibited that YL-0919 significantly inhibited the firing frequency of GABAergic neurons evoked by 250 pA current input in the presence of SB271046. $n = 8$ neurons from four mice. Data are presented as mean ± SEM. Statistics are measured by two-way ANOVA followed by Turkey's *post hoc* test (**c**) and one-way ANOVA followed by Dunnett's *post hoc* test (**d**, **e**), $^*P < 0.05$; $^{**}P < 0.01$, $^{***}P < 0.001$, $^{****}P < 0.0001$.

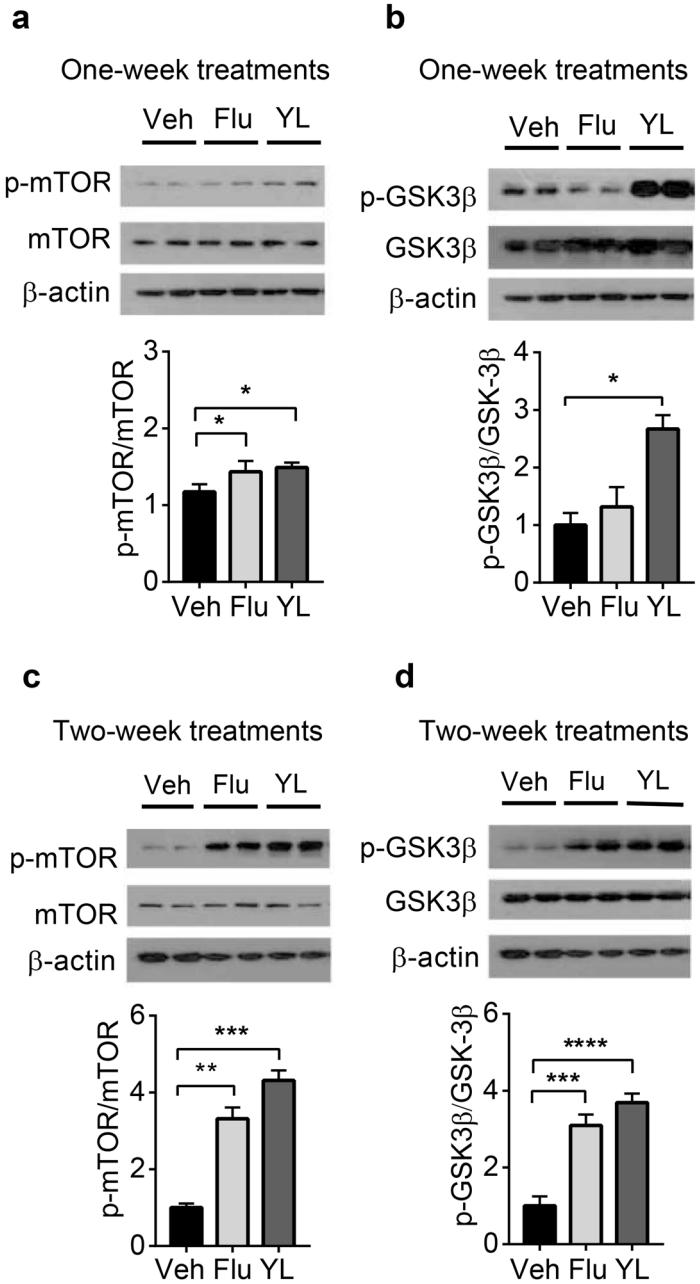

Fig. 6 YL-0919 treatment significantly increased the expression of the phosphorylation of mTOR and GSK-3β in the mPFC. a Changes of the p-mTOR and mTOR after 1-week administration of YL-0919, fluoxetine and vehicle (top); and quantified measurement of p-mTOR/mTOR expression after 1-week drug administration by densitometry (bottom); the data showed that treatment with fluoxetine and YL-0919 for 1 week significantly increased the expression of p-mTOR. **b** Changes of the p-GSK-3β and GSK-3β after 1-week administration of YL-0919, fluoxetine and vehicle; and quantified expression of p-GSK-3β/GSK-3β after 1 week of drugs administration by densitometry (bottom), the results exhibited that YL-0919 treatment for 1 week obviously increased the expression of p-GSK-3β. **c** Changes of the p-mTOR and mTOR after 2-week administration of YL-0919, fluoxetine and vehicle (top); and quantified expression of p-mTOR/mTOR after 2-week drugs administration by densitometry (bottom); the data exhibited that YL-0919 and fluoxetine significantly increased the phosphorylation of mTOR. **d** Changes of the p-GSK-3β and GSK-3β after 2-week administration of YL-0919, fluoxetine and vehicle (top); and quantified expression of p-GSK-3β/GSK-3β after 2 weeks of drugs administration by densitometry (bottom); the results showed that YL-0919 and fluoxetine treatment for 2 weeks significantly increased the phosphorylation of GSK-3β. $n = 6$ independent data, Data are presented as mean ± SEM. Statistics are measured by one-way ANOVA followed by Dunnett's *post hoc* test (**a**, **b**, **c**, **d**), $^{*}P < 0.05$; $^{**}P < 0.01$, $^{***}P < 0.001$, $^{****}P < 0.0001$.

the mPFC excitability by YL-0919 may be critical for its antidepressant effect.

Recent studies have highlighted that the GABAergic neurons played an important role for the rapid antidepressant effect. Mutant mice with deletion of the $GABA_AR$ γ2 subunit in SST interneurons resulted in disinhibition of GABA neurotransmission and produced an antidepressant-like behavior [35]. Allie et al. measured the effects of ketamine, GLYX-13 (NMDAR partial agonist), and scopolamine (the muscarinic acetylcholine receptor (mAChR) antagonist), and they found that low-dose ketamine, GLYX-13, and scopolamine reduced inhibitory input onto pyramidal cells and increased synaptic pyramidal excitability measured at

the single-cell and population levels [36]. A study from Duman's lab showed that viral-mediated knockdown of M1-AchR (M1-type muscarinic acetylcholine receptors) specifically in somatostatin (SST) interneurons, but not glutamatergic neurons in the mPFC, attenuated the rapid antidepressant-like effects of scopolamine [37]. These results suggested that GABAergic interneurons may be critical to mediate the rapid antidepressant effect targeting to Glu or ACh system, while whether monoamine antidepressants are dependent on the GABA system to exert antidepressant effects is unknown. By investigating the effect of YL-0919 on the activity of different neurons in the mPFC, we found that YL-0919 inhibited the APs of GABAergic neurons, and then generated the increase of excitatory synaptic transmission and the decrease of inhibitory synaptic transmission of mPFC.

The 5-HT_{1A} receptor is one of most important targets mediating the antidepressant effects. Early studies on the antidepressant mechanism of monoamines primarily indicated that the auto-receptors of serotonergic neurons in the presynaptic dorsal raphe nucleus and the desensitization of presynaptic 5-HT_{1A} receptors promoted the release of 5-HT in the postsynaptic brain area [38, 39]. 5-HT_{1A} receptors are abundantly distributed in post-synaptic brain regions, especially in the mPFC [40]. Many studies have reported that there is a strong link between depression and functional deficits of 5-HT_{1A} receptors in mPFC; however, the mechanism of regulation of 5-HT_{1A} receptors in the mPFC by antidepressant is unclear. Recently, Gorinski et al. found that downregulation of palmitoylation of 5-HT_{1A} receptors in the mPFC resulted in depression-like behaviors, while restoration of palmitoylation of 5-HT_{1A} receptors in mPFC exerted great potential for the treatment of major depression [41]. A study reported that cannabidiol (CBD) exerts fast and sustained antidepressant-like effects by reversing depressive behaviors in the OBX (the olfactory bulbectomy mouse model of depression), and antidepressant-like effect of CBD can be prevented by 5-HT_{1A} receptor blockade [42]. In addition, ketamine exerted antidepressant effects that lasted for 24 h and the sustained antidepressant effects were attenuated by intra-mPFC injection of a 5-HT_{1A} receptor antagonist, WAY 100635 [43]. Our investigation demonstrated that the 5-HT_{1A} receptors in the mPFC may contribute to the inhibition of GABAergic neurons by YL-0919, suggesting that 5-HT_{1A} receptor in the mPFC is important for the antidepressant effect.

Lladó-Pelfort et al. showed that intravenous injection of (±) 8-OH-DPAT (5-HT_{1A} receptor agonist) in rats exerted a preferential inhibition of GABAergic interneurons in mPFC, suggesting that 5-HT_{1A} receptors on GABAergic neurons may have a preferential response to 5-HT_{1A} agonists [40]. But their experiments were performed in vivo, lacking the neuron-specific studies. In present study, we found that YL-0919 exerted dis-inhibitory effect by preferentially acting on 5-HT_{1A} receptor distributed in GABAergic neurons. And why 5-HT_{1A} receptor on GABAergic neurons preferentially responding to YL-0919 is still an open question. The mechanism studies of ketamine showed that ketamine may preferentially inhibit the NMDA receptors on the GABAergic neurons, which also need further exploration [44]. 5-HT_{1A} receptors may exist distinct complexes with different receptors or protein molecules on different neurons. A number of studies have reported that 5-HT_{1A} receptors readily form heterodimers with other receptors (e.g., 5-HT_{2A} receptors, dopamine type 2 receptors (DRD2), fibroblast growth factor receptor 1 (FGFR1), 5-HT_7 receptors [45]), contributing to the antidepressant effect. For example, 5-HT_{1A} receptors could form heterodimers with DRD2 and mediate a different function than monomers in vitro, and activation of heterodimers in the cortex may benefit the enhancement of cognition [46]. In hippocampal and midbrain regions, 5-HT_{1A} receptors also form heterodimeric receptor complexes with brain FGFR1, and the complexes may be potential antidepressant targets [47]; in addition, 5-HT_{1A} receptors and 5-HT_7 receptors form heterodimers with high expression in brain regions associated with depression [45]. A study reported that activation of 5-HT_{1A} receptors selectively inhibits Na^+ currents in the axon initial segment of pyramidal neurons, suggesting that 5-HT_{1A} receptors on pyramidal neurons may be coupled to Na^+ channel [39]. Our results showed that YL-0919 had slight inhibition on the AP amplitude of pyramidal neurons, while strongly inhibited firing rates of AP of GABAergic neurons. Our present results indicated that YL-0919 may produce the antidepressant effect by simultaneously activating the monoamine system and the glutamate/GABA system, providing a new speculation for the development of new-generation antidepressants.

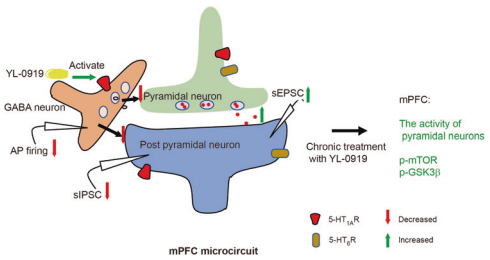

Fig. 7 Schematic hypothesis of the action of YL-0919 in mPFC microcircuit. YL-0919 preferentially activates 5-HT_{1A} receptor on GABA neurons and inhibits the membrane excitability of GABA neurons. The inhibition of GABA neurons leads to decreased inhibitory outputs to pyramidal neurons and disinhibition of glutamatergic pyramidal neurons, then adaptively increasing the excitatory inputs to pyramidal neurons. The excitability of post-synaptic pyramidal neurons is increased by increased excitatory inputs and decreased inhibitory inputs. Finally, chronic treatment with YL-0919 increased the excitability of mPFC, including the increases in activity of pyramidal neurons and the synaptic-related proteins.

Synaptic plasticity is important for the activity of mPFC. Studies on the rapid antidepressant mechanism of ketamine have reported that ketamine could rapidly activate the mTOR pathway, while inhibition of the mTOR signaling pathway could completely block the rapid antidepressant effects of ketamine, suggesting that mTOR signaling pathway may mediate the rapid antidepressant effects of ketamine [48]. Wang et al. also found that mTOR activity is related to dendritic protein synthesis, and decreased mTOR activity induced the impairment of mPFC synaptic plasticity and depressive-like behavior [49]. GSK-3β plays an important role in the regulation of learning memory, and is also involved in the mTOR-Akt-GSK-3β pathway that linked to the antidepressant effects [50, 51]. Here, we found that YL-0919 increased the phosphorylation of mTOR and GSK-3β in mPFC with a more rapid onset time than that of fluoxetine, supporting a rapid recovery of synaptic plasticity in mPFC underlying anti-depressive processes.

In conclusion, we performed multiple disciplinary experiments to reveal a novel neural mechanism in mPFC of the antidepressant YL-0919 (Fig. 7). Our results displayed that YL-0919 preferentially inhibited GABAergic neurons and reduced inhibitory input to pyramidal neurons, and 5-HT_{1A} receptor participated in the inhibition of GABA neurons. The disinhibition of GABAergic neurons may relieve the restraint of pyramidal neurons and adaptively enhance the neuronal activity of pyramidal neurons in the mPFC. Our studies indicate that 5-HT_{1A} receptor may contribute to the regulation of E/I balance related to depression, provide new evidences for the understanding of neural mechanism of monoamine antidepressants and a new reference for the development of novel antidepressants.

ACKNOWLEDGEMENTS

We thank Dr Shu-jia Zhu (Institute of Neuroscience, China) who provided the GAD-GFP mice. This work was supported by the Strategic Priority Research Program of the Chinese Academy of Sciences (XDA12040220), the National Natural Science

Foundation of China (31671049, 81773708, 81072624, and 81173036), and the National Key New Drug Creation Program of China (No. 2017ZX09309012, 2018ZX09739008, and 2018ZX09711002-002-012).

AUTHOR CONTRIBUTIONS

YL and YFL directed and supervised the project. YMZ performed experiments and analyzed data. LYY helped to produce transgenic mice and the extracellular electrophysiological recording. TYL contributed to the R-scope procedures. Fan Guo assisted with behavioral experiments. YMZ, YFL, YL, and Fei Guo designed the study and wrote and edited the manuscript.

ADDITIONAL INFORMATION

Supplementary information The online version contains supplementary material available at https://doi.org/10.1038/s41401-021-00807-0.

Competing interests: The authors declare no competing interests.

REFERENCES

1. Zhang JQ, Wu XH, Feng Y, Xie XF, Fan YH, Yan S, et al. Salvianolic acid B ameliorates depressive-like behaviors in chronic mild stress-treated mice: involvement of the neuroinflammatory pathway. Acta Pharmacol Sin. 2016;37:1141–53.
2. Chu SF, Zhang Z, Zhou X, He WB, Yang B, Cui LY, et al. Low corticosterone levels attenuate late life depression and enhance glutamatergic neurotransmission in female rats. Acta Pharmacol Sin. 2021;42:848–60.
3. Ressler KJ, Nemeroff CB. Role of serotonergic and noradrenergic systems in the pathophysiology of depression and anxiety disorders. Depress Anxiety. 2000;12 (Suppl 1):2–19.
4. Yin YY, Tian CY, Fang XX, Shang C, Zhang LM, Xu Q, et al. The faster-onset antidepressant effects of hypidone hydrochloride (YL-0919) in monkeys subjected to chronic unpredictable stress. Front Pharmacol. 2020;11:5868–79.
5. Pan SJ, Tan YL, Yao SW, Xin Y, Yang X, Liu J, et al. Fluoxetine induces lipid metabolism abnormalities by acting on the liver in patients and mice with depression. Acta Pharmacol Sin. 2018;39:1463–72.
6. Fee C, Banasr M, Sibille E. Somatostatin-positive gamma-aminobutyric acid interneuron deficits in depression: cortical microcircuit and therapeutic perspectives. Biol Psychiatry. 2017;82:549–59.
7. Li YF. A hypothesis of monoamine (5-HT) – glutamate/GABA long neural circuit: aiming for fast-onset antidepressant discovery. Pharmacol Ther. 2020;208:107494.
8. McCormack PL. Vilazodone: a review in major depressive disorder in adults. Drugs. 2015;75:1915–23.
9. Wagner G, Schultes MT, Titscher V, Teufer B, Klerings I, Gartlehner G. Efficacy and safety of levomilnacipran, vilazodone and vortioxetine compared with other second-generation antidepressants for major depressive disorder in adults:a systematic review and network meta-analysis. J Affect Disord. 2018;228:1–12.
10. Dixon ML, Thiruchselvam R, Todd R, Christoff K. Emotion and the prefrontal cortex: an integrative review. Psychological Bull. 2017;143:1033–81.
11. Warden MR, Selimbeyoglu A, Mirzabekov JJ, Lo M, Thompson KR, Kim SY, et al. A prefrontal cortex-brainstem neuronal projection that controls response to behavioural challenge. Nature. 2012;492:428–32.
12. Michelsen KA, van den Hove DL, Schmitz C, Segers O, Prickaerts J, Steinbusch HW. Prenatal stress and subsequent exposure to chronic mild stress influence dendritic spine density and morphology in the rat medial prefrontal cortex. BMC Neurosci. 2007;8:107.
13. Lee YA, Poirier P, Otani S, Goto Y. Dorsal-ventral distinction of chronic stress-induced electrophysiological alterations in the rat medial prefrontal cortex. Neuroscience. 2011;183:108–20.
14. Price RB, Duman R. Neuroplasticity in cognitive and psychological mechanisms of depression: an integrative model. Mol Psychiatry. 2020;25:530–43.
15. Pittenger C, Duman RS. Stress, depression, and neuroplasticity: a convergence of mechanisms. Neuropsychopharmacology. 2008;33:88–109.
16. McKlveen JM, Moloney RD, Scheimann JR, Myers B, Herman JP. "Braking" the prefrontal cortex: the role of glucocorticoids and interneurons in stress adaptation and pathology. Biol Psychiatry. 2019;86:669–81.
17. Hastings RS, Parsey RV, Oquendo MA, Arango V, Mann JJ. Volumetric analysis of the prefrontal cortex, amygdala, and hippocampus in major depression. Neuropsychopharmacology. 2004;29:952–9.
18. Ran YH, Hu XX, Wang YL, Zhao N, Zhang LM, Liu HX, et al. YL-0919, a dual 5-HT_{1A} partial agonist and SSRI, produces antidepressant- and anxiolytic-like effects in rats subjected to chronic unpredictable stress. Acta Pharmacol Sin. 2018;39: 12–23.
19. Chen XF, Jin ZL, Gong Y, Zhao N, Wang XY, Ran YH, et al. 5-HT_6 receptor agonist and memory-enhancing properties of hypidone hydrochloride (YL-0919), a novel 5-HT_{1A}receptor partial agonist and SSRI. Neuropharmacology. 2018;138:1–9.
20. Sun LJ, Zhang LM, Liu D, Xue R, Liu YQ, Li L, et al. The faster-onset antidepressant effects of hypidone hydrochloride (YL-0919). Metab Brain Dis. 2019;34:1375–84.
21. Zhang LM, Wang XY, Zhao N, Wang YL, Hu XX, Ran YH, et al. Neurochemical and behavioural effects of hypidone hydrochloride (YL-0919): a novel combined selective 5-HT reuptake inhibitor and partial 5-HT(1A) agonist. Br J Pharmacol. 2017;174:769–80.
22. Ran Y, Jin Z, Chen X, Zhao N, Fang X, Zhang L, et al. Hypidone hydrochloride (YL-0919) produces a fast-onset reversal of the behavioral and synaptic deficits caused by chronic stress exposure. Front Cell Neurosci. 2018;12:395.
23. Suman PR, Zerbinatti N, Theindl LC, Domingues K, Lino de Oliveira C. Failure to detect the action of antidepressants in the forced swim test in Swiss mice. Acta Neuropsychiatr. 2018;30:158–67.
24. Li Q, Zhang B, Cao H, Liu W, Guo F, Shen F, et al. Oxytocin exerts antidepressant-like effect by potentiating dopaminergic synaptic transmission in the mPFC. Neuropharmacology. 2020;162:107836.
25. Guo F, Zhang Q, Zhang B, Fu Z, Wu B, Huang C, et al. Burst-firing patterns in the prefrontal cortex underlying the neuronal mechanisms of depression probed by antidepressants. Eur J Neurosci. 2014;40:3538–47.
26. Legéndy CR, Salcman M. Bursts and recurrences of bursts in the spike trains of spontaneously active striate cortex neurons. J Neurophysiol. 1985;53:926–39.
27. Helboe L, Egebjerg J, de Jong IE. Distribution of serotonin receptor 5-HT_6 mRNA in rat neuronal subpopulations: a double in situ hybridization study. Neuroscience. 2015;310:442–54.
28. Amargós-Bosch M, Bortolozzi A, Puig MV, Serrats J, Adell A, Celada P, et al. Co-expression and in vivo interaction of serotonin1A and serotonin2A receptors in pyramidal neurons of prefrontal cortex. Cereb Cortex. 2004;14:281–99.
29. Zhou X, Zhang R, Zhang S, Wu J, Sun X. Activation of 5-HT_{1A} receptors promotes retinal ganglion cell function by inhibiting the cAMP-PKA pathway to modulate presynaptic GABA release in chronic glaucoma. J Neurosci. 2019;39:1484–504.
30. Normann C, Frase S, Haug V, von Wolff G, Clark K, Münzer P, et al. Antidepressants rescue stress-induced disruption of synaptic plasticity via serotonin transporter-independent inhibition of L-type calcium channels. Biol Psychiatry. 2018;84:55–64.
31. Cavaccini A, Gritti M, Giorgi A, Locarno A, Heck N, Migliarini S, et al. Serotonergic signaling controls input-specific synaptic plasticity at striatal circuits. Neuron. 2018;98:801–16.e7.
32. Nader K, Schafe GE, Le Doux JE. Fear memories require protein synthesis in the amygdala for reconsolidation after retrieval. Nature. 2000;406:722–6.
33. Lei Y, Wang J, Wang D, Li C, Liu B, Fang X, et al. SIRT1 in forebrain excitatory neurons produces sexually dimorphic effects on depression-related behaviors and modulates neuronal excitability and synaptic transmission in the medial prefrontal cortex. Mol Psychiatry. 2020;25:1094–111.
34. Hare BD, Shinohara R, Liu RJ, Pothula S, DiLeone RJ, Duman RS. Optogenetic stimulation of medial prefrontal cortex Drd1 neurons produces rapid and long-lasting antidepressant effects. Nat Commun. 2019;10:223.
35. Fuchs T, Jefferson SJ, Hooper A, Yee PH, Maguire J, Luscher B. Disinhibition of somatostatin-positive GABAergic interneurons results in an anxiolytic and antidepressant-like brain state. Mol Psychiatry. 2017;22:920–30.
36. Widman AJ, McMahon LL. Disinhibition of CA1 pyramidal cells by low-dose ketamine and other antagonists with rapid antidepressant efficacy. Proc Natl Acad Sci USA. 2018;115:E3007–e16.
37. Fogaça MV, Wu M, Li C, Li XY, Picciotto MR, Duman RS. Inhibition of GABA interneurons in the mPFC is sufficient and necessary for rapid antidepressant responses. Mol Psychiatry. 2021;26:3277–91.
38. Blier P, Ward NM. Is there a role for 5-HT_{1A} agonists in the treatment of depression? Biol Psychiatry. 2003;53:193–203.
39. Borroto-Escuela DO, Narváez M, Ambrogini P, Ferraro L, Brito I, Romero-Fernandez W, et al. Receptor˙receptor interactions in multiple 5-HT_{1A} heteroreceptor complexes in raphe-hippocampal 5-HT transmission and their relevance for depression and its treatment. Molecules. 2018;23:1341.
40. Lladó-Pelfort L, Santana N, Ghisi V, Artigas F, Celada P. 5-HT_{1A} receptor agonists enhance pyramidal cell firing in prefrontal cortex through a preferential action on GABA interneurons. Cereb Cortex. 2012;22:1487–97.
41. Gorinski N, Bijata M, Prasad S, Wirth A, Abdel Galil D, Zeug A, et al. Attenuated palmitoylation of serotonin receptor 5-HT1A affects receptor function and contributes to depression-like behaviors. Nat Commun. 2019;10:3924.
42. Linge R, Jiménez-Sánchez L, Campa L, Pilar-Cuéllar F, Vidal R, Pazos A, et al. Cannabidiol induces rapid-acting antidepressant-like effects and enhances cortical 5-HT/glutamate neurotransmission: role of 5-HT_{1A} receptors. Neuropharmacology. 2016;103:16–26.
43. Fukumoto K, Iijima M, Funakoshi T, Chaki S. Role of 5-HT1A receptor stimulation in the medial prefrontal cortex in the sustained antidepressant effects of ketamine. Int J Neuropsychopharmacol. 2018;21:371–81.

44. Krystal JH, Abdallah CG, Sanacora G, Charney DS, Duman RS. Ketamine: a paradigm shift for depression research and treatment. Neuron. 2019;101: 774–8.
45. Renner U, Zeug A, Woehler A, Niebert M, Dityatev A, Dityateva G, et al. Heterodimerization of serotonin receptors 5-HT_{1A} and 5-HT_7 differentially regulates receptor signalling and trafficking. J Cell Sci. 2012;125:2486–99.
46. Łukasiewicz S, Błasiak E, Szafran-Pilch K, Dziedzicka-Wasylewska M. Dopamine D2 and serotonin 5-HT_{1A} receptor interaction in the context of the effects of antipsychotics - in vitro studies. J Neurochem. 2016;137:549–60.
47. Borroto-Escuela DO, Tarakanov AO, Fuxe K. FGFR1-5-HT_{1A} heteroreceptor complexes: implications for understanding and treating major depression. Trends Neurosci. 2016;39:5–15.
48. Li N, Lee B, Liu RJ, Banasr M, Dwyer JM, Iwata M, et al. mTOR-dependent synapse formation underlies the rapid antidepressant effects of NMDA antagonists. Science. 2010;329:959–64.
49. Wang H, Huang B, Wang W, Li J, Chen Y, Flynn T, et al. High urea induces depression and LTP impairment through mTOR signalling suppression caused by carbamylation. EBioMedicine. 2019;48:478–90.
50. Ma K, Yang LM, Chen HZ, Lu Y. Activation of muscarinic receptors inhibits glutamate-induced GSK-3β overactivation in PC12 cells. Acta Pharmacol Sin. 2013;34:886–92.
51. Xu ZX, Tan JW, Xu H, Hill CJ, Ostrovskaya O, Martemyanov KA, et al. Caspase-2 promotes AMPA receptor internalization and cognitive flexibility via mTORC2-AKT-GSK3β signaling. Nat Commun. 2019;10:3622.